Journal of Structural Geology, Vol. 10, No. 4, pp. 393 to 403, 1988
Printed in Great Britain

0191-8141/88 $03.00 + 0.00
© 1988 Pergamon Press plc

Reverse fault step at Engel Peaks, Antarctic Peninsula

ALAN W. MENEILLY*

British Antarctic Survey, Natural Environment Research Council, High Cross, Madingley Road, Cambridge CB3 0ET, U.K.

(*Received* 2 *April* 1986; *accepted in revised form* 21 *December* 1987)

Abstract—A steep reverse fault at Engel Peaks, Antarctic Peninsula, cuts granophyre and overlying volcanic rocks and incorporates a lower angle zone or 'fault step'. The reverse fault step differs from the more familiar thrust ramp in that it cuts down-section in the footwall in the direction of tectonic transport. Accommodation of the fault zone to this step and its associated sidewall are discussed with reference to kinematic models for pull-apart zones and for the movement of thrust sheets over non-planar surfaces.

During movement on the main fault the step acted as a fault jog and pull-apart zone, preserving cataclasite, breccia and other structures demonstrating a brittle to ductile deformation history. Ultra-fine-grained rock in the step zone is the result of dynamic recrystallization of ultracataclasite. During episodes of brittle slip, the fault step acted as a dilational fault jog between the main steep reverse fault segments.

Rotation of mylonite into the reverse fault step and its sidewall involved flexural flow parallel to foliation. Movement of material through the step zone resulted in shear parallel to the base of the step, enhancement of breccia layering, mixing of lithologies and cleavage formation; it also involved extension at a high angle to the main movement direction to accommodate the extra length of the fault zone. Late, steep, reverse fault zones propagating from the main fault folded the breccias in the step and crenulated the earlier cleavage. The fault step was a zone of brittle dilation, hydration, diffusive mass transfer and mineralization.

INTRODUCTION

MUCH attention has been paid recently to the complex flat and ramp geometry of thrust sheets (see McClay & Price 1981 for review). The ubiquity of thrust ramps, where a thrust sheet increases its angle of climb, has prompted many analyses of the stress and strain developed during translation over a ramp (Wiltschko 1979, 1981, Berger & Johnson 1980, 1982, Fischer & Coward 1982, Sanderson 1982, Knipe 1985). Examples of thrust sheets cutting down-section in the direction of transport have also been described (e.g. Coward 1983), but are rare. In consequence there has been no attempt to describe or model the mechanics and kinematics of thrust sheets which cut down into their footwalls, except in the case of a thrust sheet moving from a ramp back to a flat (Sanderson 1982).

This paper describes the geometry, structures and microstructures of a 1 km thick reverse fault zone at Engel Peaks, NE Palmer Land, Antarctic Peninsula (Fig. 1). The ductile fault has an unusual footwall geometry (Fig. 2), defining a staircase trajectory (Rich 1934) where the steep footwall includes a lower angle zone here termed a reverse 'fault step'. A reverse fault step differs from the more familiar thrust ramp in that it cuts down-section in the footwall in the direction of tectonic transport. Kinematic analysis indicates that the main direction of tectonic transport at Engel Peaks is parallel to the footwall of the steep fault zone and that the step and the steep zone do not represent a 'flat' and 'ramp', respectively. The step therefore acts as a dilational fault jog (Sibson 1985) with related deformation mechanisms.

The Antarctic Peninsula consists of a magmatic arc built up in response to subduction of proto-Pacific ocean crust eastwards beneath the margin of Gondwanaland during most of the Mesozoic (Thomson & Pankhurst 1983, Storey & Garrett 1985, Meneilly *et al.* 1987). During the Cretaceous, increased magmatism and arc compression resulted in intense, E-directed, high-angle reverse faulting on the back-arc side of the magmatic arc (Meneilly *et al.* 1987). One such fault, at Engel Peaks, affects the Engel Peaks granophyre of 113 Ma and the

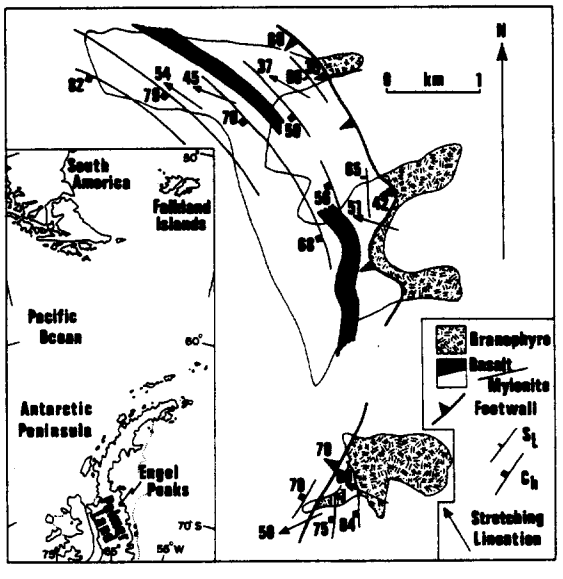

Fig. 1. Map of Engel Peaks fault zone showing trend and dip of foliation and plunge of stretching lineation. Inset shows location of Engel Peaks.

*Present address: Merlin Geophysical Ltd, Merlin House, Boundary Road, Woking, Surrey GU21 5BX, U.K.

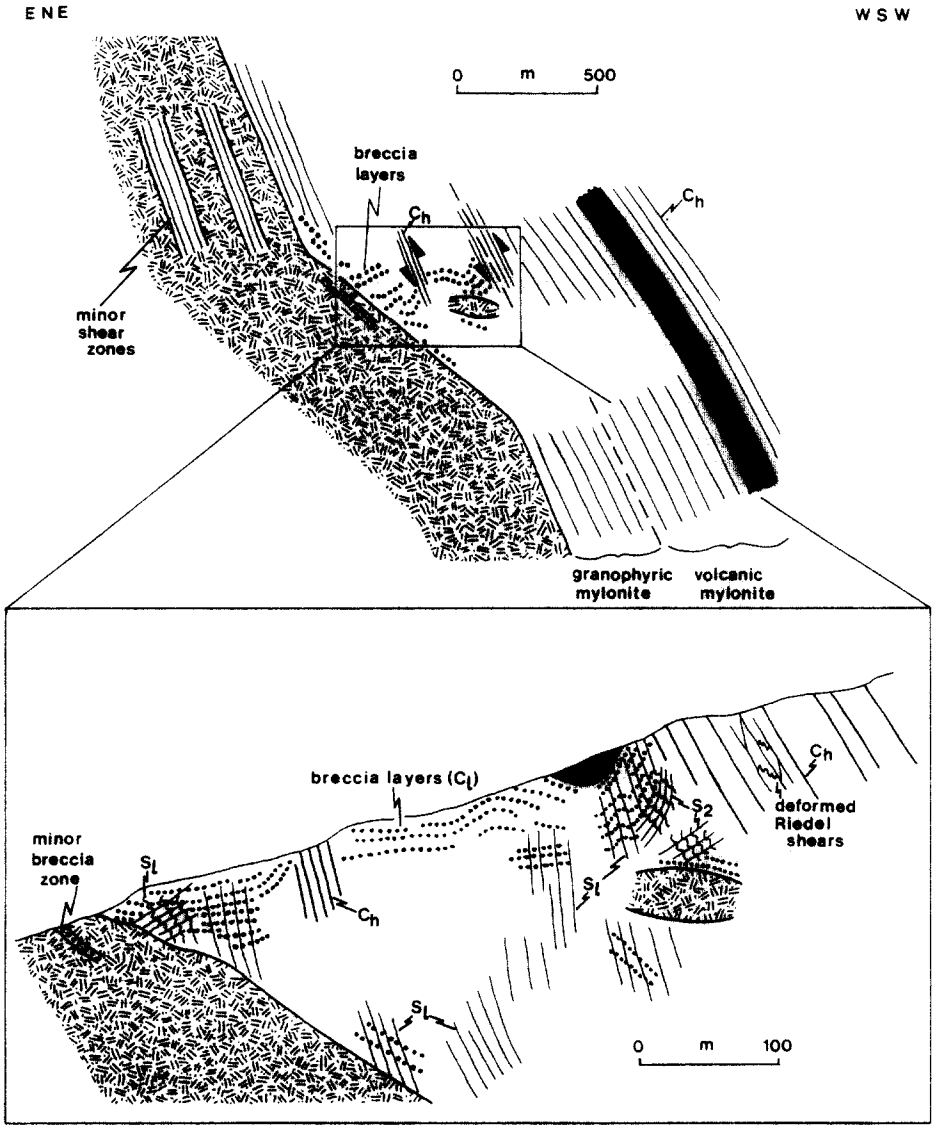

Fig. 2. Composite sketch cross-section and detail of fault step. Ornament as in Fig. 1.

older volcanic rocks into which it was intruded. The fault is a zone of ductile shear and its footwall is exposed within the granophyre. Up to 400 m of granophyre is involved in the shearing and above this are 600 m of sheared volcanic rocks, including an 80 m thick amygdaloidal metabasalt sheet (Fig. 2). Garnet in quartz veins and the mineral assemblage in metabasalt indicate that the metamorphic grade reached greenschist facies during faulting. The base of the shear zone and the main mylonitic fabric dip about 65°W (Fig. 3a). Transitions from undeformed granophyre into mylonite, where the shear foliation maintains a consistently steep dip, can be mapped at the base of the fault zone and also within shear zones up to 100 m wide in granophyre below the main fault (Fig. 2). However, in one area the footwall dips at a lower angle (42°W) and within this reverse fault step a variety of textures and structures are developed, including cataclasite, layered and folded fault breccias and a second cleavage. The step was a zone of brittle dilation and hydration and copper mineralization is widespread.

PROTOLITHS OF THE FAULT ZONE ROCKS

The Engel Peaks granophyre

This small pluton is one of many mid-Cretaceous intrusions in Palmer Land and is characterized by a variable grain size, abundance of ilmenite and a paucity of hydrous minerals. Plagioclase is present as unzoned phenocrysts up to 7 mm long and microperthitic alkali feldspar forms graphic intergrowths with quartz. Ilmenite is very abundant, accounting for 5% of some specimens and occurring as irregular, large grains or clusters of small grains, often in association with sphene and epidote. Hydrous minerals are rare and the small amounts of epidote, muscovite and stubby green biotite are probably secondary as they also occur in late quartz veins and in the mylonitized granophyre.

The Antarctic Peninsula Volcanic Group

This is a suite of calc-alkaline, mainly rhyolitic, lavas

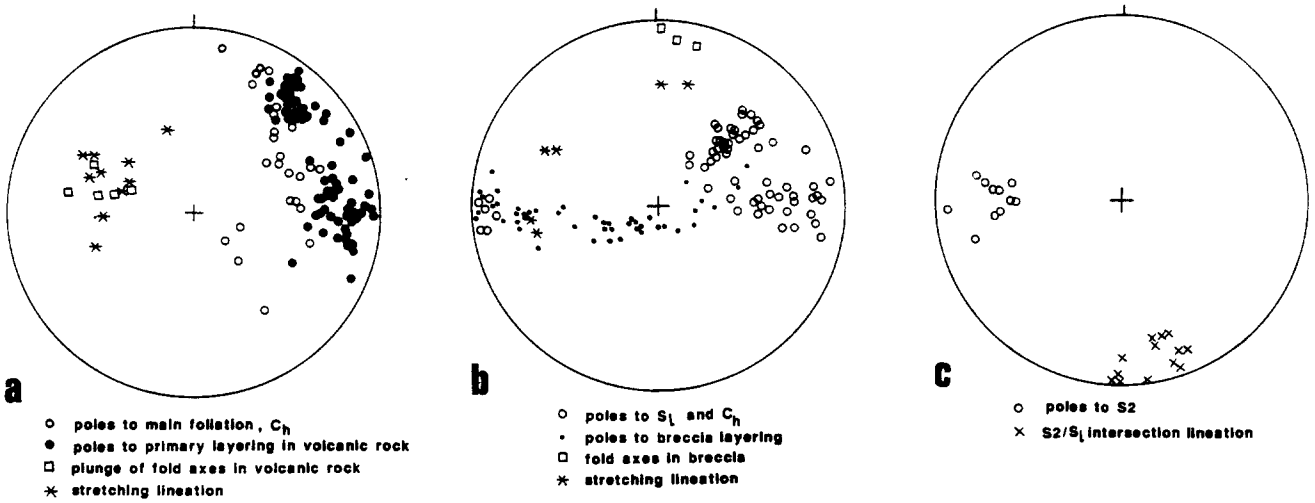

Fig. 3. Equal-area lower hemisphere projections. (a) Structures in high-angle mylonite zones. (b) and (c) Structures in fault step.

and tuffs, widespread on the Antarctic Peninsula and ranging in age from early Jurassic to Tertiary (Thomson & Pankhurst 1983). In eastern Palmer Land it includes thick (up to 1 km) amygdaloidal basalt sheets (Meneilly *et al.* 1987). The deformed rhyolitic and basaltic rocks within the Engel Peaks fault zone are probably part of this group.

MYLONITES IN THE HIGH-ANGLE FAULT ZONES

Transition into mylonitized granophyre

Transitions from undeformed granophyre to mylonite occur over distances of a few centimetres to several decimetres. Deformation commenced with anastomosing shears isolating progressively smaller relict pods of granophyre (Fig. 4a). In places these shear planes occur in two sets at 20° to, and symmetrically disposed about, the bulk shear plane. Their intersection is sub-parallel to the NW–W-plunging stretching direction, defined by stretched plagioclase phenocrysts and xenoliths, and with progressive shearing they rotated towards parallelism with the bulk shear plane. Some plagioclase phenocrysts were deformed in a semi-brittle fashion, with kinking of albite twins and boudinage, but otherwise the deformation involved dynamic recrystallization of feldspar and quartz. New quartz and feldspar grains typically have irregular, interlocking contacts and little or no crystallographic or dimensional preferred orientation. Banding is defined by zones of smaller grain size, concentration of ilmenite, mica folia and elongate pods of relict granophyre. Hydration of the granophyre and breakdown of feldspar caused growth of epidote, muscovite or biotite, and probably led to reaction enhanced ductility (White & Knipe 1978). Ilmenite was very mobile and is concentrated as small grains along fractures, grain boundaries and zones of high strain. With increasing deformation the relict granophyre pods were destroyed and a banded micaceous mylonite was produced with relict plagioclase porphyroclasts and differentiation into quartz- and mica-rich layers. Quartz recrystallized into a fine- to coarse-grained granoblastic mosaic and plagioclase also formed small, new, strain-free, euhedral or subhedral albite/oligoclase crystals on the margins of relict plagioclase from the granophyre (Fig. 4b). Indeed, some of the plagioclase crystals isolated in the mylonites may be porphyroblasts rather than relict porphyroclasts.

Within the steep, W-dipping mylonite zone there is a simple relationship between the fault zone footwall and the main mylonite foliation which both lie sub-parallel to the inferred bulk shear plane. Between microscopic shear planes (main foliation) an oblique preferred orientation of mica, and occasionally quartz, is interpreted as being parallel to the direction of finite elongation in that microlithon. The main foliation and the oblique mica fabric thus represent the *C* and *S* planes respectively of Berthé *et al.* (1979) and consistently indicate thrust sense towards the east (Fig. 4c). The main foliation (*C* planes) in the high-angle mylonite zone is designated C_h and the oblique fabric (*S* planes) S_h.

Sheared volcanic rocks

The contact between the Engel Peaks granophyre and the older volcanic sequence is difficult to detect in the field. The granophyre has been reduced to a porphyroclastic mylonite containing relict plagioclase crystals and small new albite porphyroblasts. The sheared rhyolite is also a porphyroclastic mylonite with relict plagioclase and quartz phenocrysts in a matrix of recrystallized quartz, feldspar and mica which is indistinguishable from the granophyric mylonite matrix. Large, embayed quartz crystals in the rhyolitic mylonites distinguish them from the granophyric mylonites. Occasionally primary layering in volcanic rocks dips west at a slightly lower angle than C_h and rare folds plunge WNW, sub-parallel to stretching (Fig. 3a).

The amygdaloidal metabasalts within the volcanic sequence consist of biotite, actinolitic hornblende,

albite, epidote and quartz with stretched amygdales filled with quartz, epidote and calcite. Undeformed basalt has almost spherical amygdales which make excellent strain markers (Fig. 4d). The shape fabric of 224 amygdales in five specimens indicate approximately plane strain ellipsoids. Assuming simple shear deformation the measured axial ratios suggest a shear strain of approximately 3.5. This can be taken as a minimum for the bulk shear strain in the fault zone because strains in the micro-crystalline (grain size <20 μm) granophyric and rhyolitic mylonites are likely to have been much higher.

STRUCTURES WITHIN THE FAULT STEP

The lower-angle fault step does not have the simple *SC* planes of the high-angle mylonite zones, but contains a variety of brittle and ductile fault rocks including cataclasite, breccia and ultramylonite. The following structures are found within the step (Figs. 2 and 3b & c).

(1) Gently inclined layered breccias were initially sub-parallel to the base of the step and to the local shear direction (see discussion below) and are designated C_l (*C* planes in the lower-angle zone). They were subsequently folded about steep W-dipping axial planes.

(2) A generally weak but penetrative primary cleavage, S_l (*S* planes in the lower-angle zone), dips steeply to the west.

(3) Zones of intense shear parallel to those in the W-dipping, high-angle mylonite zones (C_h) cut and fold the breccias.

(4) A crenulation cleavage (S_2) dipping moderately or steeply to the east is sporadically developed, but is stronger within the late, high-angle shear zones.

(5) An area of steep SSW-dipping foliation occurs at the northernmost exposures of the fault (Fig. 1). This domain underwent late dextral shear with en échelon tension gashes parallel to foliation and is interpreted as the side-wall to the fault step.

Evidence for shear sense at the base of the step is rare but minor crystal offsets, and primary cleavage (S_l) dipping steeply to the west, indicate E-directed thrusting parallel to the step footwall. S_l abuts against undeformed granophyre at the base of the step at an angle of 30–40° (Fig. 2). Thus, S_l is not a plane of shear and although sub-parallel to it in places, is not the C_h shear foliation of the steep mylonite zone. Where C_h is present within the step it causes marked rotation of breccia layering into steep shear zones (Fig. 2).

Breccias at the base of the step were produced by both brittle and ductile processes. Cataclasites are invariably affected by later recrystallization or ductile deformation. Some breccias with an ultra-fine-grained, random-fabric matrix are interpreted to be recrystallized ultracataclasite.

Brittle fractures at the fault step margin

In patches at the base of the fault step the granophyre is shattered and cut by reticulate meso-fractures 10 μm–0.5 cm wide (Fig. 5a & b), which are marked by concentrations of ilmenite and sparse, small, new muscovite flakes. The wider fracture zones consist of thin, ilmenite-lined cracks and fine, recrystallized quartz and feldspar with disseminated ilmenite grains. The granophyre between the fractures is weakly deformed with kinkbands and fractures in plagioclase phenocrysts and undulatory extinction and subgrain formation in quartz and feldspar. The granophyre appears to have been initially fractured and then partially recrystallized, especially along fracture planes.

Recrystallized ultracataclasite at the fault step margin

At the base of the step is a patchily developed zone (up to 2 m thick) of nearly structureless, ultra-fine-grained, recrystallized granophyre, containing rounded to angular fragments of relict granophyre. Large blocks of the plutonic rock are isolated in the recrystallized areas and are cut by discontinuous 'veins' and patches of it. Similar, irregular patches and discontinuous 'veins' of the recrystallized rock also occur in the granophyre within a few metres of the overlying fault (Fig. 5c). In thin section the dark, recrystallized areas consist of very fine-grained quartz and feldspar with serrated, interlocking boundaries 10 μm across (Fig. 5d) together with finely disseminated ilmenite grains. Much of this microcrystalline, random-fabric rock shows evidence of crystal–plastic deformation processes only and the rock appears to have been frozen at the stage of dynamic recovery following intense grain refinement.

It is usually impossible to deduce the complete deformation mechanism path through which a rock has passed. In many cases only the very latest, and possibly minor, strain increment is recorded by the microstructures and there may be no clues as to the dominant deformation mechanism operating during the main fabric-forming strain history. At Engel Peaks, however, textures transitional between the granophyre and the ultra-fine-grained rock suggest a two stage, brittle to ductile deformation sequence resulting in a dynamically recrystallized ultracataclasite. In the brittly fractured granophyre, described in the previous section, recrystallization of cataclasite occurred along fracture planes in zones up to 0.5 cm wide. The texture within these fracture zones is very similar to that of the ultra-fine-grained rock; fine, serrated, equidimensional quartz and feldspar grains and tiny disseminated ilmenite grains. Ilmenite is concentrated along the meso-fractures (Fig. 5b). In the ultra-fine-grained rock angular granophyre fragments and ghost reticulate fractures defined by planes of ilmenite concentration are evidence of a brittle precursor to the now pervasively recrystallized granophyre. White *et al.* (1982) concluded that many mylonites probably began as cataclasites: dilation allowed ingress of water and reaction softening leading to ductile mylonitization. Superplastic flow was likely to have been an important process in the fault step once the small grain size was established by cataclasis. White

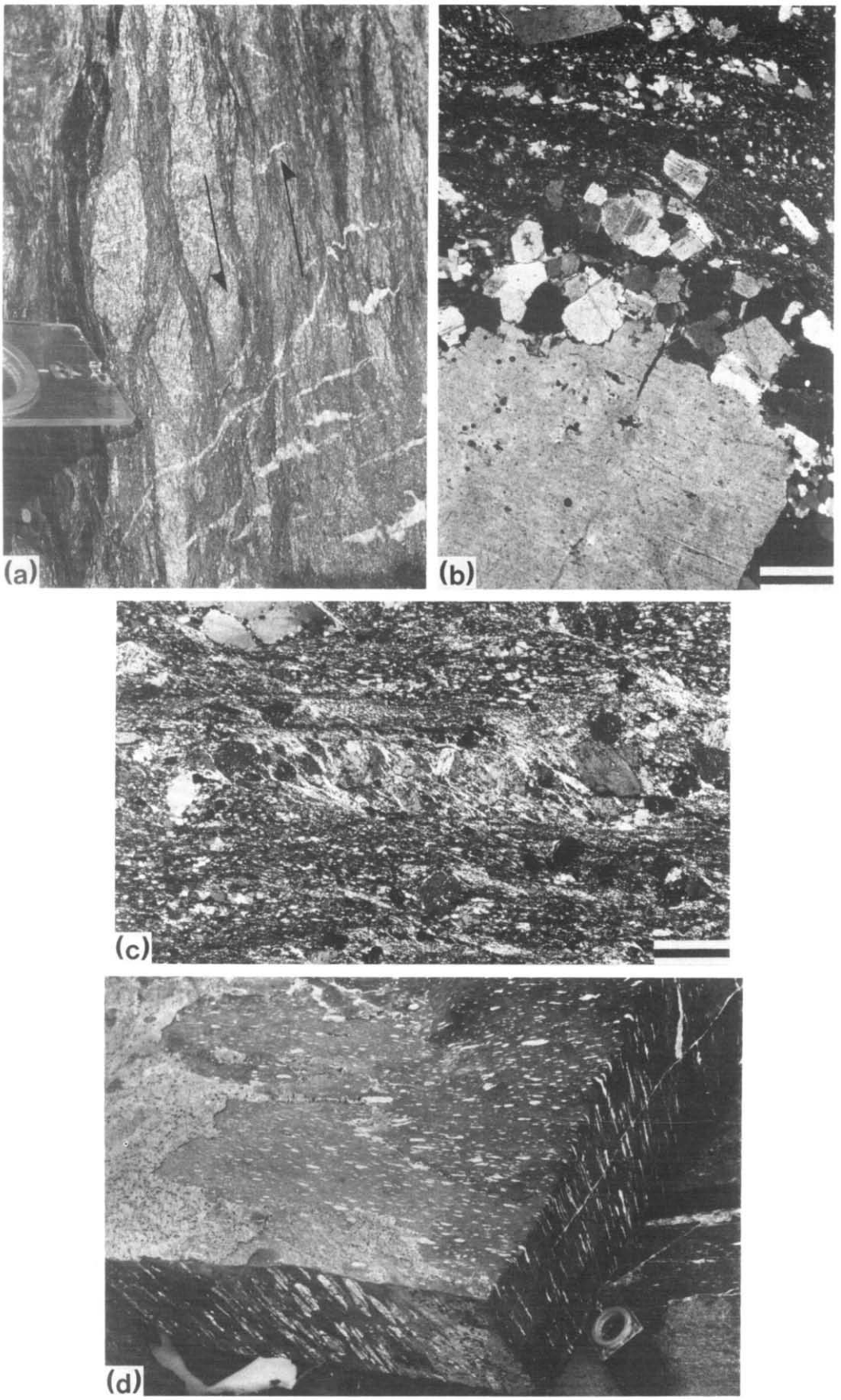

Fig. 4. (a) Anastomosing mylonite zones in vertical exposure of granophyre. Sense of shear, recognized from curve of foliation into mylonite zones, is thrusting towards the left (east). (b) Small, new plagioclase grains on the margin of plagioclase porphyroclast in mylonite. Scale bar 0.5 mm. Cross-polarizers. (c) *C* and *S* planes (indicating sinistral shear in the photograph) from mylonite. Scale bar 0.5 mm. Cross-polarizers. (d) Deformed amygdaloidal basalt with joint surfaces sub-parallel to the three principal planes of the strain ellipsoid.

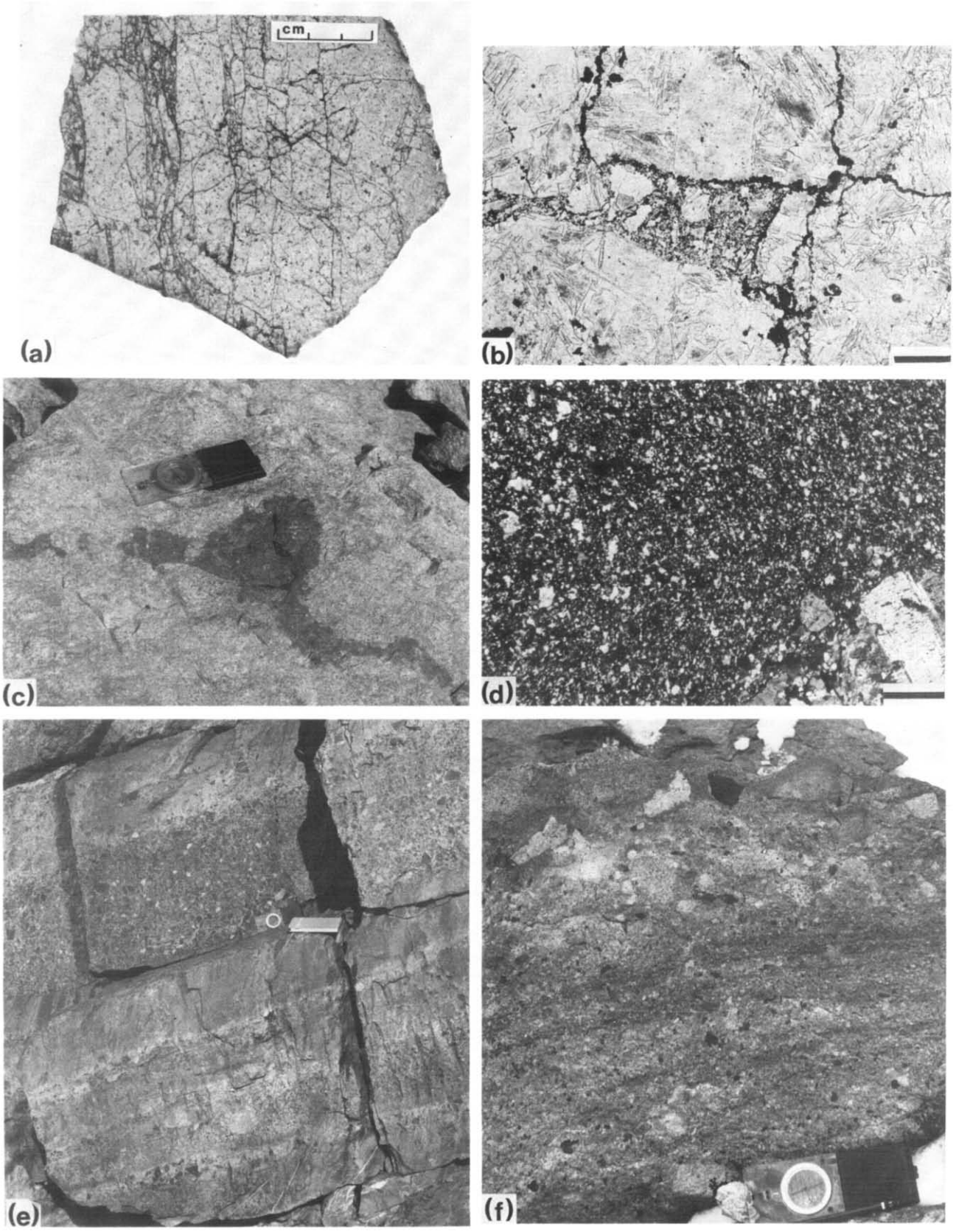

Fig. 5. (a) Reticulate fractures in granophyre. (b) Thin section of cataclasite in granophyre. Note concentration of opaque ilmenite along fractures. Scale bar 0.5 mm. Plane-polarized light. (c) Patch of ultra-mylonite in granophyre one metre below the base of the step. (d) Ultramylonite. Note fine grain size, serrated grains and relict granophyre fragment at lower right. Scale bar 0.5 mm. Cross-polarizers. (e) Layered fault breccia dipping to the east. Light fragments are granophyre, dark fragments are of volcanics and mylonite. (f) Detail of breccia layer with a predominance of granophyre fragments and finer-grained, darker laminae. Note gradation between granophyre clasts and matrix.

(1976) and White *et al.* (1980) conclude that superplastic behaviour is favoured by high initial stress, grain size less than 100 μm and the presence of a dispersed second phase inhibiting grain growth. These conditions are all features of the ultramylonite in the fault step with the fine, disseminated ilmenite grains inhibiting grain growth. This process results in a fine-grained cataclasite with a weak or random fabric. The grain refinement does not always accommodate significant mesoscopic strain. This is evident from its common occurrence as irregular patches in granophyre below the main fault plane (Fig. 5c). This fact, and the lack of a well-developed foliation, supports the proposition of cataclasis as the initial mechanism of grain size reduction.

Layered breccias

Above the marginal, random-fabric fault rocks is a zone of interlayered breccias and porphyroclastic mylonites about 100 m thick (Fig. 5e & f). Layered breccias reach a thickness of 40 m with individual layers from microscopic scale up to 1 m. They superficially resemble conglomerates or agglomerates and were previously described as the former by Davies (1984). Field and textural evidence strongly suggests, however, that they were formed during faulting by brittle and ductile deformation of granophyre, identical to that recognized in the marginal, random-fabric fault rocks into which they merge.

The matrix of the breccias consists of fine- or very-fine-grained, equidimensional, serrated, interlocking quartz and feldspar crystals with fine, disseminated ilmenite grains and patches of epidote or sphene and variable amounts of fine muscovite and green biotite. The 'clasts' consist of variably dynamically recrystallized granophyre, basalt, rhyolitic volcanic rock and, most significantly, fragments of ultra-fine-grained, recrystallized granophyre. This last component was generated during earlier grain refinement (see previous section) and has subsequently been incorporated into polylithic breccias during continued disintegration and mixing of lithologies at the granophyre–volcanic rock contact. Large fragments of rhyolite up to 1.5 m across and a large pod of granophyre 50 m across have survived intact 50 m above the base of the fault step (Fig. 2).

The fine matrix of the breccias shows little sign of crystallographic or dimensional preferred orientation and there is little evidence of strain within much of the breccias in the form of augen structures or stretched clasts. This could be due to the very fine grain size (20 μm) of the matrix promoting grain-boundary sliding and superplasticity, leaving the rigid clasts unstrained. Muscovite and green biotite flakes generally have a strong preferred orientation parallel to breccia layering, even where quartz and feldspar have a random fabric. These mica folia, and very-fine-grained, ilmenite-rich layers (Fig. 5f), suggest shear parallel to breccia layering. In places the breccias have a superimposed pervasive E-dipping ductile cleavage (S_1) with muscovite folia and stretched lithic fragments with quartz-filled strain shadows. However, even in the most foliated breccias, the quartz and feldspar develop only a very weak elongation, suggesting that continual deformation and dynamic recrystallization to small equant grains plus grain-boundary sliding were still the dominant deformation mechanisms.

INTERACTION OF BRITTLE AND DUCTILE DEFORMATION

Breccias in the fault step

It has been shown how initial brittle deformation at the base of the fault step was followed by ductile dynamic recrystallization of breccia matrix and subsequently by pervasive ductile flow of matrix and lithic clasts. This progression from brittle to ductile processes can be explained by a change in the physical conditions within a particular body of rock with time. The following factors could have played a role in this transition:

(i) increase in temperature due to shear heating (Brun & Cobbold 1980, Scholz 1980) and convective fluid transfer (Beach 1976);

(ii) hydration of the initially 'dry' Engel Peaks granophyre could have led to hydrolytic weakening of quartz (Tullis & Yund 1980) and to growth of micas causing reaction enhanced ductility (White & Knipe 1978);

(iii) once ductile deformation has commenced it may be self perpetuating because it initiates strain softening processes which localize the deformation, for example, continual recrystallization, geometric softening, grain-boundary sliding and superplasticity (see White *et al.* 1980 for review);

(iv) changing thermal regime due to upward transport of hotter rock in the hangingwall.

Ductile–brittle–ductile sequence in rhyolitic mylonites in the steep fault zone

Rhyolitic mylonites in the shear zone centre resulted from ductile shearing similar to that which affected the granophyric mylonites in the steep fault zone. In places the foliation in the rhyolitic mylonite is cut by two or three sets of brittle fractures along which ilmenite is concentrated. Ilmenite also segregated along cleavage adjacent to the fractures. One fracture set is parallel to the main penetrative cleavage (C_h), another dips at a shallower angle to the west and is usually folded, and the third is vertical and unfolded. Figure 6 illustrates how this arrangement could be due to a Riedel shear fracture system which has been deformed by resumed ductile shear with the same E-directed thrusting sense.

This punctuation by brittle deformation in the ductile flow of the rhyolitic mylonites could be due to one or more of many possible changes in the physical and chemical conditions within the shear zone. Three possible histories are suggested:

(i) work hardening in quartz and feldspar during

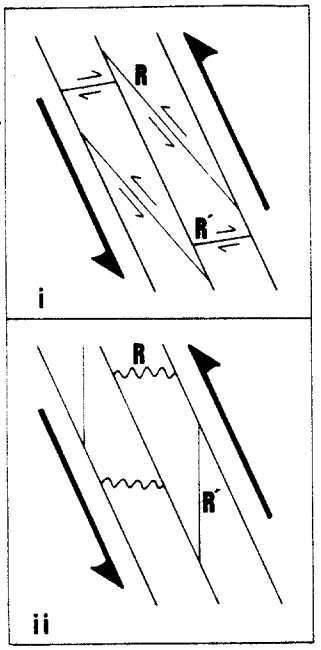

Fig. 6. Riedel shears (i), deformed by resumption of ductile shear (ii). *R* shear fractures are shortened and folded whilst *R'* fractures are extended.

tile deformation could change the rheology of the rock and provoke brittle failure. This could then allow the introduction of more fluid into the system causing a reversion to crystal–plastic deformation. The process could be repeated cyclically in a fault zone as suggested by White *et al.* (1982);

(ii) transport of the mylonites to higher crustal levels and consequent lowering of temperature and normal stress could cause brittle deformation leading to hydration and return to ductile behaviour;

(iii) aseismic shearing could be interrupted by propagating earthquake ruptures (Sibson 1980). This possibility is discussed further below.

ACCOMMODATION OF THE FAULT ZONE TO THE STEP

The simple *SC* fabric of the high-angle mylonite zones suggests that the main fault movement at Engel Peaks is a steep, E-directed ductile reverse fault. A cross-section (Fig. 2) shows that the fault step links two zones of high-angle shear. It is possible that the steep fault zone at Engel Peaks is part of a large-scale ramp on a major low-angle thrust approximately parallel to the footwall of the fault step. However, if this were the case then structures due to rotation of the thrust sheet into the ramp should be present in the steep mylonite zones and the main tectonic transport direction would be parallel to the footwall of the step. It will be demonstrated that the textures and structures within the step are all fault rock fabrics accommodating approximately simple shear parallel to the main high-angle ductile reverse fault.

Whatever the origin of the stepped footwall there are two important mechanical consequences of accommodation to a fault step (Figs. 7 and 8).

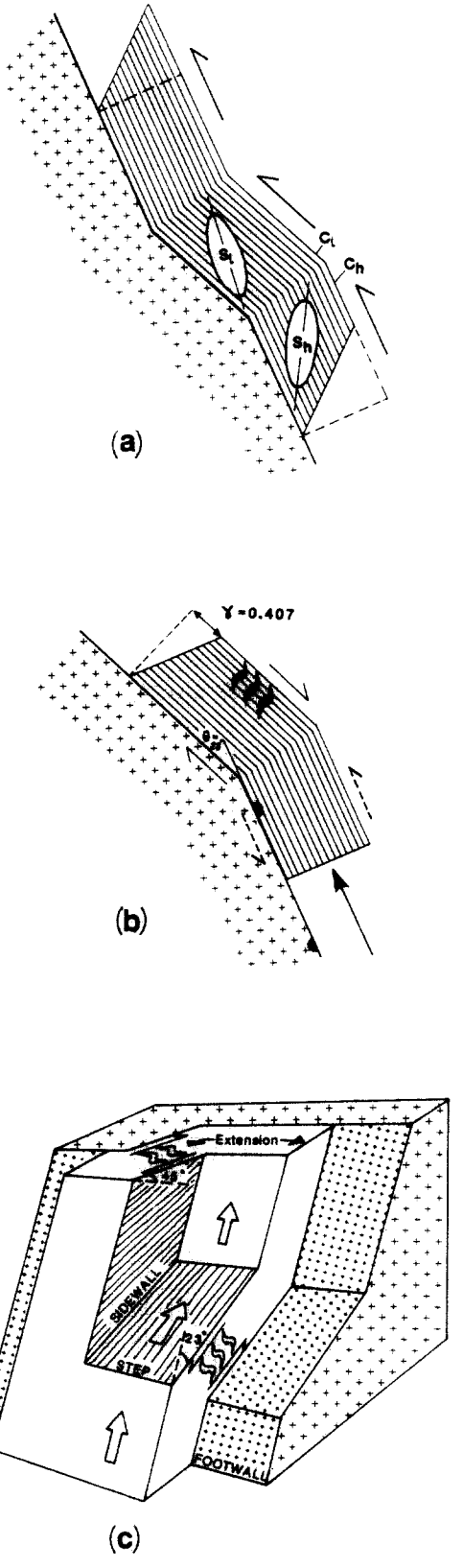

Fig. 7. (a) Movement of thrust sheet over step by flow parallel to footwall (*C* planes) and without décollement. (b) Flexural flow (solid shear direction symbols) to accommodate rotation of thrust sheet into step (after Sanderson 1982). Shear within the thrust sheet in the direction of tectonic transport (dashed shear direction symbols) is not considered but, if present, will decrease amount of reverse flexural flow. (c) Schematic block diagram of Engel Peaks fault step and associated sidewall (viewed from the SW). Dextral shear parallel to foliation due to flexural flow as fault rocks enter sidewall and extension of step and sidewall to accommodate extra length of fault zone.

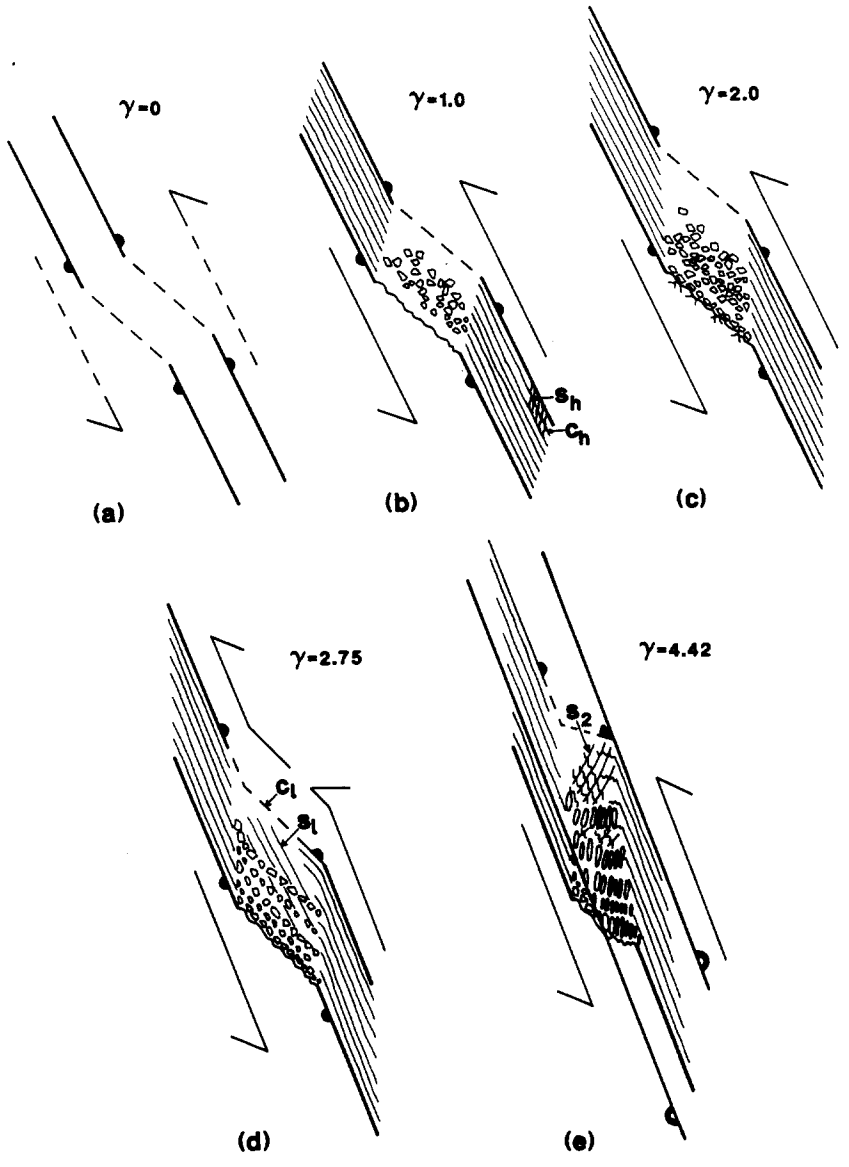

Fig. 8. Evolution of reverse fault step at Engel Peaks. Shear strain (γ) in steep mylonite zones given. (a) Step between two high-angle reverse fault segments. The step may be a channel for passive flow of material or a zone of extension linking the steep segments. (b) Displacement on steep faults generates linking zone of extension (dilational fault jog) and brecciation in strain shadow of fault step. (c) Increase in width of the fault zone will cause more wall rocks to be incorporated into the step as breccia layers. (d) Ductile flow of material around the step by shear parallel to its footwall enhances breccia layering (C_l) and produces cleavage (S_l). (e) Steep mylonite zone widens and propagates into step, shearing and folding breccia layers and crenulating S_l and the rotated C_h.

(1) If the bounding walls to the fault zone remain rigid, displacement parallel to the high-angle fault segments will cause extension in the step parallel to the shear direction. This extension is akin to a 'pull-apart' linking two segments of a strike-slip fault (Burchfiel & Stewart 1966).

(2) The fault zone rocks must deform internally if they rotate into and out of the step.

Strain shadow in the fault step preserving early cataclastic fabric

The pull-apart zone in the fault step would have been a strain shadow within the major high-angle reverse fault, analogous to a releasing bend in a strike-slip system (Crowell 1974). The strain shadow preserves the early cataclastic fabric and the history of brittle to ductile deformation mechanisms. Widening of the fault zone may have incorporated more wall rocks into the step zone as breccia layers (Fig. 8c).

Sibson (1985) described 'dilational fault jogs' linking segments of high-level strike-slip faults in which fault breccias form by implosion during the rapid slip transfer across the jog accompanying earthquake ruptures on the main fault. Cataclasis in the fault step at Engel Peaks could, at least in part, be related to such rapid slip transfer across the fault step. The Riedel shear fracturing interrupting the ductile flow in the steep mylonite zones may represent such brittle slip episodes external to the dilational fault jog. Evidence of more extensive brittle deformation within the steep mylonites would have been destroyed by the subsequent superimposed ductile

shear. The breccia layering in the step zone may be related to successive earthquake ruptures along the major fault.

Movement of thrust sheets over non-planar surfaces

Shear parallel to the breccia layering in the reverse fault step indicates that it was not purely a zone of dilational pull-apart. The step was also utilized as a zone of shear linking the two steep thrust segments (Fig. 8d) and accommodated flow of material through the fault step. The primary cleavage (S_l) at about 40° to the fault step base (Fig. 2b) is consistent with easterly directed thrusting parallel to the contact. Layer parallel shear enhanced the layering in the breccias (Fig. 5f) and may have folded those layers originally dipping at a lower angle to the west. The ductile mylonites at the highest structural level exposed at Engel Peaks bend through the step and the main mylonite foliation (C_h) dips at a lower angle (Fig. 2).

Sanderson (1982) presented two simple models for the deformation of a thrust sheet as it passes over a ramp. The models involve décollement above an undeformed footwall without internal deformation of the thrust sheet by shear in the direction of tectonic transport during thrusting. At Engel Peaks there is, in places, a transition into mylonite at the base of the fault, suggesting that continuity across the shear zone was preserved and there may have been no décollement. A model for rotation of a thrust sheet without décollement is illustrated by the example of the Engel Peaks reverse fault (Fig. 7a). Translation is accomplished by flow parallel to the footwall (C plane) and the inflexion plane migrates through the mylonites (cf. migration of a fold hinge during rotation of the axial plane). Cleavage (S planes) recording the finite XY plane dip to the west at a shallower angle in the step (S_l) than in the high-angle zone (S_h).

Sanderson's (1982) flexural flow ramp model examined the strain recorded in a thrust sheet with no internal shear in the direction of tectonic transport. This model predicts that mylonite entering the fault step from the steep reverse fault zone undergoes flexural flow parallel to C_h in a sense opposite to the tectonic transport direction (Fig. 7b). In Sanderson's model the shear strain parallel to C_h is given by:

$$\gamma = 2 \tan (\theta/2),$$

where θ is the angle through which the thrust sheet is rotated. For a maximum rotation at Engel Peaks of 23° (Fig. 7b) the shear strain will be approximately 0.4. At the northern end of Engel Peaks, late, sigmoidal, quartz-filled tension gashes indicate reversal of shear approximately parallel to the early stretching direction. This agrees with the flexural flow model and suggests some décollement at the base, or within the thrust sheet. If, as is likely at Engel Peaks, shear in the direction of tectonic transport was still taking place then the resultant reverse shear strain would be less than 0.4.

A map of the fault zone (Fig. 1) shows that the main cleavage, C_h, which is approximately parallel to the bulk shear plane, swings anticlockwise to dip steeply SSW at the northern end of the exposure. Within this SSW-dipping domain late dextral shear took place, resulting in en échelon, sigmoidal, quartz-filled tension gashes. This domain is interpreted as a sidewall to the fault step (Fig. 7c). The flexural flow model of Sanderson (1982) predicts dextral shear parallel to C_h on rotation of the fault zone mylonites into the sidewall and this is supported by the field evidence. Extension parallel to C_h is found in the step where clasts in the breccias have been extended along a horizontal N–S axis normal to the transport direction. Extension parallel to a thrust front has been discussed in relation to differential thrust transport by Coward & Kim (1981) and Sanderson (1982). A similar mechanism is proposed here for the Engel Peaks fault zone which is extended on entering the fault step (Fig. 7c). For rotation of the mylonite zone through 45° into the sidewall of the step at Engel Peaks (Fig. 7c) Sanderson's model predicts a maximum shear strain parallel to C_h of 0.83.

SUMMARY AND CONCLUSIONS

(1) The Engel Peaks reverse fault is a steep, ductile, shear zone incorporating a lower angle slip transfer zone or reverse fault step with its associated sidewall. The reverse fault step differs from the more familiar thrust ramp in that it cuts down-section in the footwall in the direction of tectonic transport.

(2) During movement on the main high-angle fault the step acted as a dilational fault jog or pull-apart zone. Whether the step was an original feature of the footwall or whether it linked two en échelon steep reverse fault segments, dilation was necessary to accommodate movement between a rigid footwall and hangingwall. The step zone was a strain shadow which preserves cataclastic fabrics and a history of brittle to ductile deformation mechanisms.

(3) Brecciation episodes in the ductile flow of mylonites within the steep zones may have been caused by earthquake ruptures propagating along the main steep reverse fault. The step zone would have acted as a dilational fault jog allowing slip transfer between steep fault segments and possibly preserving evidence of slip episodes as breccia layers.

(4) Ultra-fine-grained rock in the step probably resulted from a combination of early cataclasis and later ductile deformation resulting in a dynamically recrystallized ultracataclasite. During the crystal–plastic stage superplastic flow of the fine-grained rock hindered development of foliation or preferred orientation.

(5) Movement of fault rocks through the thrust step zone resulted in shear parallel to the footwall of the step, enhancement of breccia layering, mixing of lithologies and cleavage formation (S_l).

(6) Rotation of mylonite from the steep reverse fault into the step involved flexural flow parallel to foliation in

the opposite sense to the bulk shear. Rotation of mylonite into the sidewall of the step also resulted in flexural flow.

(7) Movement of fault rocks into the step involved extension approximately normal to the main tectonic transport direction to accommodate the extra horizontal length of the fault zone.

(8) Propagation of steep shear zones from the main steep reverse fault into the step resulted in folding of breccia layers and crenulation of S_1.

(9) The fault step model, developed here for steep reverse faults should also have useful applications to thrust zones and normal faults. One situation in which pull-apart is likely to take place in dip-slip faults is where a ramped thrust is reactivated as a normal fault and the ramps become normal fault steps and zones of dilation (C. Ferguson, personal communication).

(10) A fault step is a zone of brittle dilation, hydration and diffusive mass transfer. It is thus likely to be a site of alteration and mineralization and at Engel Peaks quartz-veining and copper mineralization are widespread. Stepped thrust faults have been recognized as zones of enhanced structural permeability and mineralization by Johnston *et al.* (1985).

Acknowledgements—I thank Bryan Storey for encouragement and discussion and for critically reading the manuscript. I also thank my colleagues at the British Antarctic Survey, especially Phil Marsh, Alistair Moyes and John Smellie, for useful discussions. Comments from two anonymous referees substantially improved the paper.

REFERENCES

Beach, A. 1976. The interrelations of fluid transport, deformation, geochemistry and heat flow in early Proterozoic shear zones in the Lewisian complex. *Phil. Trans. R. Soc.* **A280**, 569–604.

Berger, P. & Johnson, A. M. 1980. First-order analysis of deformation of a thrust sheet moving over a ramp. *Tectonophysics* **70**, T9–T24.

Berger, P. & Johnson, A. M. 1982. Folding of passive layers and forms of minor structures near terminations of blind thrust faults—application to the central Appalachian blind thrust. *J. Struct. Geol.* **4**, 343–353.

Berthé, D., Choukroune, P. & Jegouzo, P. 1979. Orthogneiss, mylonite and non-coaxial deformation of granites: the example of the South Armorican Shear Zone. *J. Struct. Geol.* **1**, 31–42.

Brun, J. P. & Cobbold, P. R. 1980. Strain heating in shear zones. *J. Struct. Geol.* **2**, 149–158.

Burchfiel, B. C. & Stewart, J. H. 1966. "Pull-apart" origin of the central segment of Death Valley, California. *Bull. geol. Soc. Am.* **77**, 439–442.

Coward, M. P. 1983. The thrust and shear zones of the Moine thrust zone and the NW Scottish Caledonides. *J. geol. Soc. Lond.* **140**, 795–811.

Coward, M. P. & Kim, J. H. 1981. Strain within thrust sheets. In: *Thrust and Nappe Tectonics* (edited by McClay, K. R. & Price, N. J.). *Spec. Publs geol. Soc. Lond.* **9**, 275–292.

Crowell, J. C. 1974. Sedimentation along the San Andreas Fault. In: *Modern and Ancient Geosynclinal Sedimentation* (edited by Dott, R. H.). *Spec. Publs Soc. econ. Paleontol. Mineral. Tulsa* **19**, 292–303.

Davies, T. G. 1984. The geology of part of Northern Palmer Land. *Scient. Rep. Br. Antarct. Surv.* **103**.

Fischer, M. W. & Coward, M. P. 1982. Strains and folds within thrust sheets: an analysis of the Heilam sheet, northwest Scotland. *Tectonophysics* **88**, 291–313.

Johnston, J. D., Wall, V. J. & Etheridge, M. A. 1985. Why unconformity related U deposits are unconformity related (abstract). *J. Struct. Geol.* **7**, 494.

Knipe, R. J. 1985. Footwall geometry and the rheology of thrust sheets. *J. Struct. Geol.* **7**, 1–10.

McClay, K. R. & Price, N. J. (Eds). 1981. *Thrust and Nappe Tectonics. Spec. Publs geol. Soc. Lond.* **9**.

Meneilly, A. W., Harrison, S. M., Piercy, B. A. & Storey, B. C. 1987. Structural evolution of the magmatic arc in Northern Palmer Land, Antarctic Peninsula. In: *Gondwana Six: Structure, Tectonics and Geophysics* (edited by McKenzie, G. D.). *Am. Geophys. Un., Geophys. Monogr.* **40**, 209–219.

Ramsay, J. G. 1967. *Folding and Fracturing of Rocks.* McGraw-Hill, New York.

Rich, J. L. 1934. Mechanics of low-angle overthrust faulting illustrated by Cumberland Thrust Block Virginia, Kentucky and Tennessee. *Bull. Am. Ass. Petrol. Geol.* **18**, 1584–1596.

Sanderson, D. J. 1982. Models of strain variation in nappes and thrust sheets: a review. *Tectonophysics* **88**, 201–235.

Scholz, C. H. 1980. Shear heating and the state of stress on faults. *J. geophys. Res.* **85**, 6174–6184.

Sibson, R. H. 1980. Transient discontinuities in ductile shear zones. *J. Struct. Geol.* **2** 165–171.

Sibson, R. H. 1985. Stopping of earthquake ruptures at dilational fault jogs. *Nature, Lond.* **316**, 248–251.

Storey, B. C. & Garrett, S. W. 1985. Crustal growth of the Antarctic Peninsula by accretion, magmatism and extension. *Geol. Mag.* **122**, 5–14.

Thomson, M. R. A. & Pankhurst, R. J. 1983. Age of post-Gondwanian calc-alkaline volcanism in the Antarctic Peninsula region. In: *Antarctic Earth Science* (edited by Oliver, R. L., James, P. R. & Jago, J. B.). Australian Academy of Science, Canberra, 328–333.

Tullis, J. & Yund, R. A. 1980. Hydrolytic weakening of experimentally deformed Westerly granite and Hale albite rock. *J. Struct. Geol.* **2**, 439–451.

White, S. 1976. The effects of strain on the microstructures, fabrics, and deformation mechanisms in quartzites. *Phil. Trans. R. Soc. Lond.* **A283**, 69–86.

White, S. H., Burrows, S. E., Carreras, J., Shaw, N. D. & Humphreys, F. J. 1980. On mylonites in ductile shear zones. *J. Struct. Geol.* **2**, 175–187.

White, S. H., Evans, D. J. & Zhong, D.-L. 1982. Fault rocks of the Moine Thrust zone: microstructures and textures of selected mylonites. *Textures and Microstructures* **5**, 33–61.

White, S. H. & Knipe, R. J. 1978. Transformation- and reaction-enhanced ductility in rocks. *J. geol. Soc. Lond.* **135**, 513–516.

Wiltschko, D. V. 1979. Mechanical model for thrust sheet deformation at a ramp. *J. geophys. Res.* **84**, 1091–2204.

Wiltschko, . V. 1981. Thrust sheet deformation. In: *Thrust and Nappe Tectonics* (edited by McClay, K. R. & Price, N. J.). *Spec. Publs geol. Soc. Lond.* **9**, 55–63.